Proceedings of the 28th IEEE
EMBS Annual International Conference
New York City, USA, Aug 30-Sept 3, 2006

In Vivo RF Powering for Advanced Biological Research

Mark D. Zimmerman, Nattapon Chaimanonart, and Darrin J. Young

Abstract—**An optimized remote powering architecture with a miniature and implantable RF power converter for an untethered small laboratory animal inside a cage is proposed. The proposed implantable device exhibits dimensions less than 6 mm x 6 mm x 1 mm, and a mass of 100 mg including a medical-grade silicon coating. The external system consists of a Class-E power amplifier driving a tuned 15 cm x 25 cm external coil placed underneath the cage. The implant device is located in the animal's abdomen in a plane parallel to the external coil and utilizes inductive coupling to receive power from the external system. A half-wave rectifier rectifies the received AC voltage and passes the resulting DC current to a 2.5 kΩ resistor, which represents the loading of an implantable microsystem. An optimal operating point with respect to operating frequency and number of turns in each coil inductor was determined by analyzing the system efficiency. The determined optimal operating condition is based on a 4-turn external coil and a 20-turn internal coil operating at 4 MHz. With the Class-E amplifier consuming a constant power of 25 W, this operating condition is sufficient to supply a desired 3.2 V with 1.3 mA to the load over a cage size of 10 cm x 20 cm with an animal tilting angle of up to 60°, which is the worst case considered for the prototype design. A voltage regulator can be designed to regulate the received DC power to a stable supply for the bio-implant microsystem.**

I. Introduction

DNA sequencing of a small laboratory animal together with *in vivo* real-time biological information, such as blood pressure, temperature, activity and bio-potential signals, is ultimately crucial for various biomedical and genetic research to identify genetic variation susceptibility to diseases, i.e. hypertension, obesity, epilepsy and cancers [1], and to potentially develop new treatments for diseases. A small-size, light-weight, long-term, reliable bio-sensing implant system with two-way wireless telemetry capability is highly desirable to capture the real-time biological information from a "free" roaming animal housed in its home cage as shown in Figure 1. However, the implant system must be minimally invasive to avoid physiological and behavioral side effects, which can distort the detected signals. Current commercial products, while able to capture some biological information, are insufficient for long term research due to large size and weight, which causes significant post-implant trauma, thus distorting the biological data. In these implants, the large size and weight are associated with the system power supply—often a heavy battery or a large inductor coil. The use of low-power integrated circuits and MEMS sensors in the proposed implantable bio-sensing microsystem significantly reduces the overall system power consumption, thus allowing a miniature coil inductor to be employed to convert RF power to a DC voltage to supply the microsystem using a highly efficient external power amplifier.

The paper is organized as follows. Section II introduces the overall system architecture and discusses the selected power amplifier design. Section III describes the methods used for system analysis and optimization. Measurement results are presented in section IV, with conclusions drawn in Section V.

Manuscript received April 3, 2006. This work was supported in part by the National Science Foundation under contract # EIA-0319811 and Case Prime Fellowship from Case School of Engineering at Case Western Reserve University.

The authors are with the Department of Electrical Engineering, Case Western Reserve University, Cleveland, OH 44106 USA. (e-mail: mark.zimmerman@case.edu)

II. Proposed System Architecture

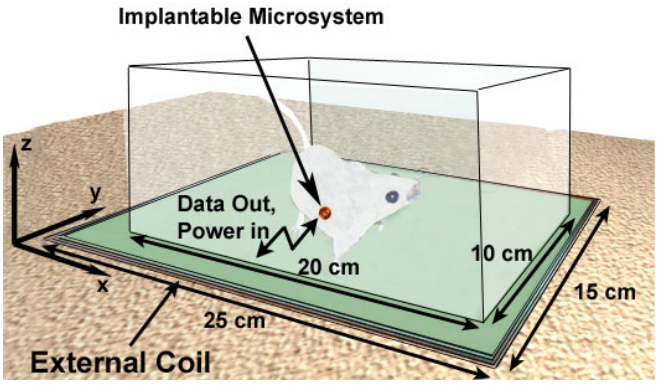

Fig. 1. Overall System Architecture

Figure 1 presents the overall system architecture. The *in vivo* microsystem employs a micro-fabricated sensor array for multi-channel vital signals monitoring and integrated electronics for sensor interfacing, RF powering and two-way data telemetry. The microsystem is wrapped by a miniature wire coil, which is inductively coupled with an external coil loop exhibiting dimensions slightly larger than the cage. A power amplifier driving the external coil for RF powering is not shown in the figure. The system will be presented in four parts: the external coil, the inductive coupling, the power amplifier, and the internal coil.

A. External Coil

A single large coil loop as in Figure 1 is chosen as a desirable approach as opposed to a grid of smaller coils in an attempt to minimize coupling variations over the

operating region [2]. The small coils provide stronger inductive coupling but introduce drastic coupling variations at coil boundaries, significantly increase the temperature of the cage floor, and require complex control electronics. The proposed large coil architecture moves the coupling variation and temperature increase to the edges of the coil and thus outside the operating region. However, the low coupling between the coils in this architecture reduces efficiency and thus requires a significant system optimization to achieve a feasible RF powering system.

B. Inductive Coupling

A simplified inductive RF powering architecture is presented in Figure 2.

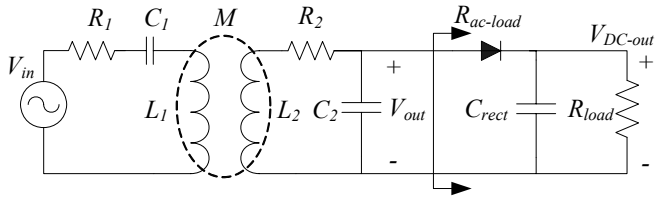

Fig. 2. Remote RF Powering Architecture

The system consists of a power source, V_{in}, driving the external coil, L_1, tuned with C_1. The mutual inductance, M, between L_1 and the internal coil, L_2, couples RF power to the tank formed by L_2 and C_2, tuned to the same frequency. R_1 and R_2 represent the equivalent series resistance (ESR) associated with the external and internal coils, respectively. The half-wave rectifier then delivers a DC power to the implantable microsystem, represented by R_{load}. In this paper, "V_{out}" refers to the AC voltage before the rectifier and "$V_{DC\text{-}out}$" refers to the DC voltage after the rectifier. The half-wave rectifier presents an equivalent AC resistance to the parallel tank, $R_{ac\text{-}load}$, which can be expressed as

$$R_{ac-load} = R_{load} / 2 . \tag{1}$$

The voltage gain expression from V_{in} to V_{out} can be expressed as [3]

$$\frac{V_{out}}{V_{in}} = \frac{\omega^2 L_2 M}{R_1 R_2 + (\omega M)^2 + R_1 \dfrac{(\omega L_2)^2}{R_{ac-load}}}, \tag{2}$$

where ω represents the tuned operating frequency. This expression will be used for system analysis and optimization as will be outlined in section III.

C. Power Amplifier

The Class-E amplifier, diagrammed in Figure 3, is chosen due to its near-zero output resistance and near-zero power loss. The only output resistance seen by the resonant network is the channel resistance of the switching transistor M_1—less than 1 Ω for the device selected. The amplifier

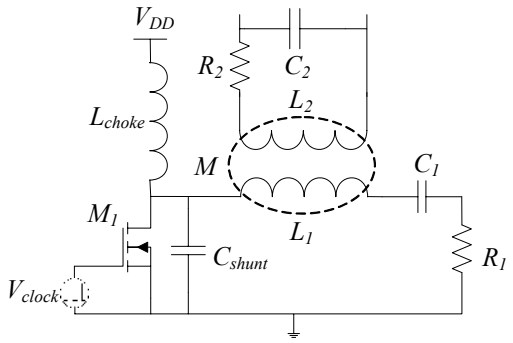

Fig. 3. Class-E Power Amplifier Schematic

achieves the near-zero power loss while operating in what is known as Zero Voltage Switching (ZVS) mode [4]. When component values are properly chosen, the voltage at the drain of M_1 is brought to zero immediately before the switch closes by the action of the resonant network and shunt capacitor. Figure 4 shows the measured drain voltage and clock waveforms of a properly tuned Class-E amplifier. In this figure, the transistor is on when V_{clock} is high. Minimal current is drawn through the transistor in this setup, thus minimizing power dissipation across the switching transistor. In testing, efficiencies—defined as the ratio of power transferred to R_1 to power drawn from the supply—of up to 98% are achieved.

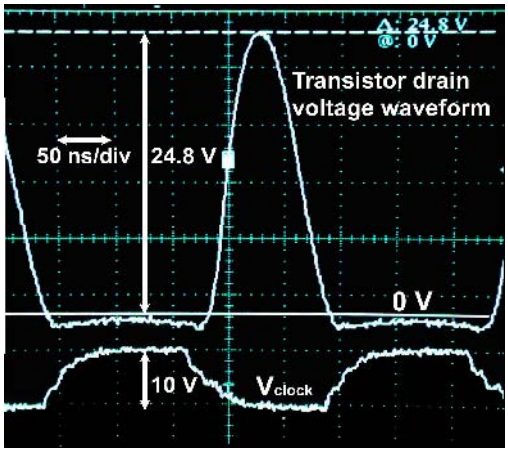

Fig. 4. Measured Class-E Amplifier Zero Voltage Switching Operation versus Input Clock Waveform

D. Internal Coil

Wrapping the coil around the silicon IC maximizes the size and shape advantages of using an integrated microsystem. Figure 5 shows a commercial rectifier diode in the center of the coil loop for initial testing purposes. In the final system design, the diode will be integrated as a part of the implantable microsystem. This planar configuration yields a number of benefits—including a 20x decrease in mass and a 30x decrease in volume—over commercial products, such as the VitalView by Minimitter [5].

RF power is coupled to the planar coil by magnetic field lines perpendicular to the coil plane. The external coil

produces a vertical magnetic field over the majority of its area, thus the planar coil is best implanted in the abdomen of the laboratory animal, close to and parallel to the external coil. This means, however, that less power is coupled to the internal coil when the animal stands up and the magnetic field is no longer perpendicular to the coil plane.

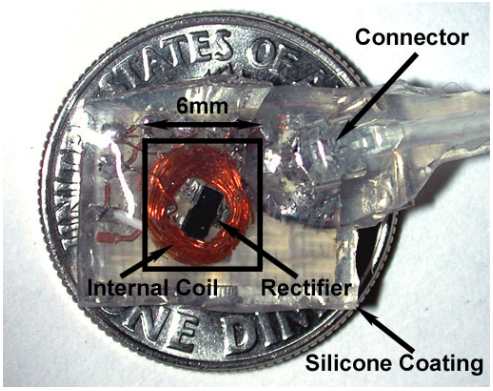

Fig. 5. Prototype Implantable Device Encased in Bio-Compatible Silicone Coating (shown with U.S. dime for size comparison)

III. Analysis And Optimization

The goal of the system optimization process is to find the most efficient operating point—defined as the highest ratio of power transferred to $R_{ac\text{-}load}$ versus power consumed by the Class-E amplifier—for the system as a function of number of turns in the internal coil, number of turns in the external coil, and operating frequency. The efficiency of the amplifier and the efficiency of the coupling between the coils can be analyzed separately and then combined to find the most efficient operating point.

The coupling constant, k, is a factor that defines the strength of the magnetic interaction between the two coils. The mutual inductance between the two inductors is dependent upon the inductances of both coils as well as this coupling constant and can be determined as

$$M = k\sqrt{L_1 L_2}\ . \tag{3}$$

If the component values in the linear circuit shown in Figure 2 are known, measuring the output from a known source allows the calculation of the mutual inductance by rearranging (2). From M, the coupling constant k can be determined from (3). The coupling constant is dependent only upon the shape, size, and orientation of the coils. Being independent to the first order of component values, frequency, number of turns in coils, etc., k is thus essential for simulations and predictions of system performance. Experiments reveal k to be 0.0017 for the following alignment: internal coil located at the center of external coil (x = 12.5 cm, y = 7.5 cm) with 1 cm spacing and 0° tilt (parallel). This location is used for the prediction and testing of system efficiency due to the stability of k near this location for small spatial displacements. The 1 cm spacing simulates the expected average distance between the implanted device and the external coil. From the measured k, performance can be predicted for all characterized inductors at any operating frequency.

Defining the efficiency of the linear system, η_c, as the ratio of power received by $R_{ac\text{-}load}$ to power drawn from V_{in} and applying (2), the following equation for the coupling efficiency can be derived:

$$\eta_c \approx \frac{\frac{V_{out}^{\ 2}}{R_{ac-load}}}{\frac{V_{in}^{\ 2}}{R_1}} = \left(\frac{\omega^2 M L_2}{R_1 R_2 + (\omega M)^2 + R_1 \frac{(\omega L_2)^2}{R_{ac-load}}} \right)^2 \frac{R_1}{R_{ac-load}} \tag{4}$$

Power losses from the Class-E amplifier can then be approximated by using equations from Kazimierczuk's and Czarkowski's Resonant Power Converters [4]. Adapting the terms for this particular situation yields the following expression for the efficiency of the amplifier, defined as the ratio of power received by the $L_1C_1R_1$ resonant network to power drawn from the V_{DD} supply

$$\eta_a = 1 - \frac{8r_{L-choke}}{(\pi^2+4)R_1} - \frac{(\pi^2+28)r_{DS}}{2(\pi^2+4)R_1} - \frac{(\pi^2-4)r_{C-shunt}}{2(\pi^2+4)R_1} - \frac{(\omega t_f)^2}{12}, \tag{5}$$

where $r_{L\text{-}choke}$ is the resistance of the choke inductor, r_{DS} is the drain resistance of the switching transistor, $r_{C\text{-}shunt}$ is the resistance of the shunt capacitor, and t_f is the fall time of the transistor. Of these terms, the second term dominates for frequencies under 10 MHz for an r_{DS} value of 0.35 Ω.

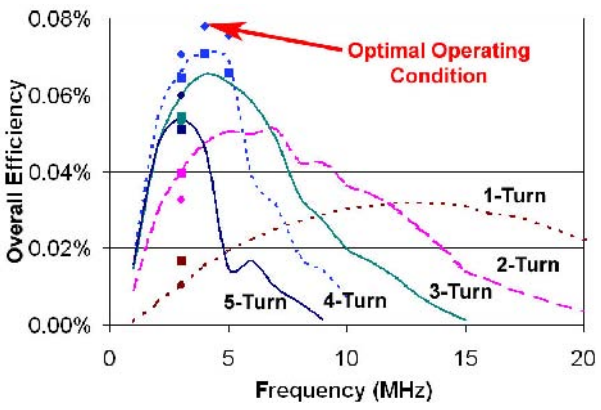

Fig. 6. Overall Efficiency Predictions and Measurement Results for 20-Turn Internal Coil (Diamond indicates measurement; square indicates simulation result; line indicates mathematical prediction.)

The overall predicted efficiency is the product of the coupling efficiencies of η_c and η_a. The overall efficiency values are obtained for internal coils with 15, 20, 25, and 30 turns, and external coils with 1, 2, 3, 4, and 5 turns over the operating frequency range of 1 MHz to 20 MHz.

Measurements are taken under a variety of conditions to confirm the calculations. The highest efficiency is found to occur with the 20-turn internal coil and 4-turn external coil operated at 4 MHz as shown in Figure 6. Under these operating conditions, component values are L_1 = 13.2 µH, L_2 = 2.6 µH, R_1 = 7.0 Ω, and R_2 = 2.53 Ω.

Figure 6 shows the trend for efficiency predicted from Equations (4) and (5). Equation (4) suggests that efficiency should increase with increasing frequency. Conversely, the ESR of any inductor increases with frequency due to skin effect and self resonant effects, causing the efficiency to decrease. Thus, we expect to see a peak efficiency frequency for each inductor from the interplay of these two effects.

The optimal operating conditions yield a measured efficiency of 0.09 % under an $R_{ac\text{-}load}$ of 1.25 kΩ when the internal coil is positioned above the middle of external coil with zero-degree tilt. This efficiency is limited by the low k value of 0.0017, which limits the coupling efficiency η_c.

IV. Measurement Results

The system characterization test setup is as depicted in Figure 1. The 4-turn external coil is driven at 4 MHz by a properly tuned Class-E amplifier, and the voltage, V_{out}, is measured across the 20-turn internal coil with a vertical (z-axis) separation of 1 cm at numerous positions over the external coil's surface. From these values, and knowing the input power to the system, the measured efficiency can be calculated for each point. Knowing the efficiency for a point, the output power and thus output voltage can be calculated for any given input power.

Due to thermal effects, the Class-E amplifier can support a maximum sustained power consumption of 25 Watts without a reduction in efficiency. The worst-case coupling for which the system is designed is the internal coil at a 60° tilt at the center of the external coil and with 1 cm vertical spacing. The efficiency at this point was measured to be 0.02 %. Using the 25 W input power and the 0.02 % efficiency, the worst-case power delivered to the internal LC tank is found to be 5.1 mW, which in turn results in 1.3 mA DC current flowing through the DC load resistance of 2.5 kΩ.

Figure 7 shows the DC output voltage, $V_{DC\text{-}out}$, across an R_{load} of 2.5 kΩ with 25 Watts drawn by the Class-E amplifier both as predicted from the previously mentioned efficiencies and as measured in actual trials. Operating only between X=2.5 cm to X=22.5 cm [as indicated by the vertical bars on the graphs] eliminates the low and high coupling zones. A similar analysis along the Y direction yields similar results. The necessary 3 V_{DC} (indicated by the horizontal bar) can be sustained over this entire region. Coupling between the inductors, and thus the expected $V_{DC\text{-}out}$, decreases to zero as the tilting angle approaches 90°. Reference [2] shows that, for this application, *in vivo* voltage measurements are essentially the same as the external measurements at the chosen operating frequency. Therefore, the results obtained from the current experiments can be used as a design guideline for the ultimate *in vivo* system development.

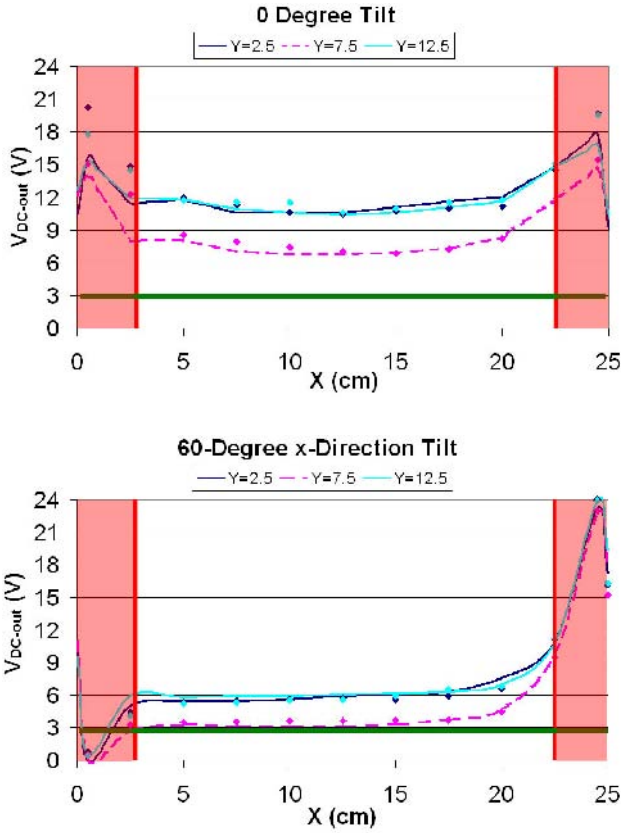

Fig. 7. DC Output Voltage ($V_{DC\text{-}out}$ from Figure 2) versus Internal Coil Position and Tilting Angle. (Diamond indicates measurement; line indicates prediction.)

V. Conclusion

In conclusion, a miniature and implantable RF powering system for long-term *in vivo* biological monitoring is proposed. Over a cage size of 10 cm x 20 cm, at a separation distance of 1 cm from an external coil, and for a tilting angle of up to 60°, the objective of supplying a DC voltage of 3 V with 1.3 mA to an implantable microsystem can be realized.

References

[1] B. Hoit, *et al*., "Naturally Occurring Variation in Cardiovascular Traits among Inbred Mouse Strains," *Genomics*, Vol. 79, no. 5, May 2002, pp. 679-685.

[2] N. Chaimanonart, *et al*., "Implantable RF Power Converter for Small Animal In Vivo Biological Monitoring," *IEEE Engineering in Medicine and Biology Society*, September 2005, pp. 1159-1562.

[3] N. Chaimanonart, W. H. Ko, and D. J. Young, "Remote RF Powering System for MEMS Strain Sensors," *Technical Digest of The Third IEEE International Conference on Sensors*, October 2004, pp. 1522-1525.

[4] M. K. Kazimierczuk and D. Czarkowski, "Class E Zero-Voltage-Switching Resonant Inverter," in *Resonant Power Converters*, New York: John Wiley & Sons, Inc., 1995, pp. 347-377.

[5] "VitalView No-Battery Telemetric Transponder System," MiniMitter Inc., [Online] Available: http://www.minimitter.com/Products/VitalView/Series4000.html